Molecular Biology of the Cell
Vol. 18, 1480–1489, April 2007

A Phenomics Approach in Yeast Links Proton and Calcium Pump Function in the Golgi[D]

Jyoti Yadav, Sabina Muend, Yongqiang Zhang, and Rajini Rao

Department of Physiology, The Johns Hopkins University School of Medicine, Baltimore, MD 21205

Submitted November 29, 2006; Revised January 26, 2007; Accepted February 1, 2007
Monitoring Editor: Vivek Malhotra

The Golgi-localized Ca^{2+}- and Mn^{2+}-transporting ATPase Pmr1 is important for secretory pathway functions. Yeast mutants lacking Pmr1 show growth sensitivity to multiple drugs (amiodarone, wortmannin, sulfometuron methyl, and tunicamycin) and ions (Mn^{2+} and Ca^{2+}). To find components that function within the same or parallel cellular pathways as Pmr1, we identified genes that shared multiple *pmr1* phenotypes. These genes were enriched in functional categories of cellular transport and interaction with cellular environment, and predominantly localize to the endomembrane system. The vacuolar-type H^+-transporting ATPase (V-ATPase), rather than other Ca^{2+} transporters, was found to most closely phenocopy *pmr1*Δ, including a shared sensitivity to Zn^{2+} and calcofluor white. However, we show that *pmr1*Δ mutants maintain normal vacuolar and prevacuolar pH and that the two transporters do not directly influence each other's activity. Together with a synthetic fitness defect of *pmr1*Δ*vma*Δ double mutants, this suggests that Pmr1 and V-ATPase work in parallel toward a common function. Overlaying data sets of growth sensitivities with functional screens (carboxypeptidase secretion and Alcian Blue binding) revealed a common set of genes relating to Golgi function. We conclude that overlapping phenotypes with Pmr1 reveal Golgi-localized functions of the V-ATPase and emphasize the importance of calcium and proton transport in secretory/prevacuolar traffic.

INTRODUCTION

A family of ATP-powered pumps drive the uphill transport of Ca^{2+} across membranes to maintain resting cytosolic Ca^{2+} at submicromolar levels as a prerequisite for ubiquitous and diverse signaling events essential to biology, such as sperm motility, fertilization, T-cell activation, synaptic vesicle fusion, and muscle contraction, to name a few. One such Ca^{2+}-ATPase localizing to the Golgi is evolutionarily conserved from yeast to mammals, and it plays a critical role in secretory pathway functions, including protein processing, sorting, and glycosylation. A unique property of the secretory pathway Ca^{2+}-ATPase (SPCA) is that it also transports Mn^{2+} with high affinity, serving the dual function of Mn^{2+} detoxification via exocytosis and providing Mn^{2+} for Golgi-localized enzymes such as Kex2 protease and mannosyltransferases (Ton *et al*., 2002). Disruption of one allele of *ATP2C1*, encoding human SPCA1, leads to Hailey Hailey disease (HHD), an ulcerative skin disorder characterized by disruption of desmosomal contacts in keratinocytes (Foggia and Hovnanian, 2004). Whereas the molecular etiology of the disease is not clear, it is thought that in HHD patients abnormally high cytosolic ion concentrations, abnormally low luminal ion concentrations, or both, could lead to defective expression, modification, and trafficking of desmosomal proteins. Homozygous null mutations in *ATP2C1* seem to be inviable in mammals, although they are tolerated in lower eukaryotes, including fungi and *Caenorhabditis elegans* (Rudolph *et al*., 1989; Cho *et al*., 2005), where compensatory mechanisms presumably suffice to allow viability. A particularly tractable model for understanding such mechanisms is the *Saccharomyces cerevisiae* orthologue Pmr1 (for review, see Ton and Rao, 2004). The identification of diverse *pmr1* mutant phenotypes in yeast has been invaluable in guiding studies on metazoan SPCA orthologues (e.g., see Cho *et al*., 2005; Ramos-Castaneda *et al*., 2005), although we cannot yet understand the complex network of gene interactions that lead to many of these phenotypes, including HHD in human. The use of ion-supplemented media (Durr *et al*., 1998) and ion-selective Pmr1 mutants (Mandal *et al*., 2000), provides the opportunity to distinguish between Ca^{2+}- and Mn^{2+}-specific phenotypes.

Conventional genome-wide approaches have identified global patterns of gene expression (transcriptome), physical interactions between gene products (proteome), gene interactions (e.g., synthetic lethal screens), and enzyme function (metabolome). By analogy, the phenome describes genome-wide phenotypic profiles, usually of growth. Herein, we analyze the yeast phenome to find pathways and genes relating to the cellular function of Pmr1. We found that any single phenotypic screen of the haploid yeast deletion collection elicited a broad response, with genes functioning in diverse pathways, making it difficult to discern the underlying gene network leading to the common phenotype with *pmr1*Δ. In contrast, the subset of genes sharing multiple, overlapping phenotypes with *pmr1*Δ was highly enriched in distinct functional categories and subcellular localization. Unexpectedly, this approach did not identify other Ca^{2+} transporters, pointing to a unique, nonredundant role for

This article was published online ahead of print in *MBC in Press* (http://www.molbiolcell.org/cgi/doi/10.1091/mbc.E06–11–1049) on February 21, 2007.

[D] The online version of this article contains supplemental material at *MBC Online* (http://www.molbiolcell.org).

Address correspondence to: Rajini Rao (rrao@jhmi.edu).

Abbreviations used: BAPTA, 1,2-bis(2-aminophenoxy)ethane-*N*,*N*,*N*′,*N*′-tetraacetic acid; BPS, bathophenanthroline disulfonate; CPY, carboxypeptidase Y; FM4-64, N-(3-triethylammoniumpropyl)-4-(*p*-diethylaminophenyl-hexatrienyl) pyridinium dibromide; VPS, vacuolar protein sorting.

Golgi-localized ion homeostasis. Instead, mutants of the vacuolar-type H^+-transporting ATPase (V-ATPase) were found to most closely phenocopy *pmr1*Δ. Although it is established that the V-ATPase is found in multiple compartments, including the Golgi (Manolson *et al*., 1994; Kawasaki-Nishi *et al*., 2001), it has not yet been possible to distinguish between organelle-specific functions, and most *vma* phenotypes in yeast are attributed to a vacuolar function by default. Our findings lead us to propose that shared phenotypes of *vma* mutants with *pmr1*Δ, including multidrug and ion sensitivity, are evidence for Golgi-localized functions of the V-ATPase. We suggest that this simple approach of overlapping multiple, distinct phenotypes can be applied to any gene to reveal new insights into cellular function.

MATERIALS AND METHODS

Yeast Strains, Growth Screens, and Analysis

A library of 4828 *S. cerevisiae* strains with deletion of each nonessential gene in a haploid background (BY4742; *MATα*) was purchased from Research Genetics (ResGen; Invitrogen, Carlsbad, CA). Each strain has a complete replacement of one open reading frame with the *kanMX* cassette. To make double knockouts, replacement of the *PMR1::kanMX* cassette with the *NAT* marker was made in the BY4741 background (*MATa*) as described previously (Tong *et al*., 2001), and the resulting strain mated with *vma2*Δ, *vma5*Δ or *snf6*Δ from the BY4742 collection. Diploids were selected on YPD plates supplemented with both 200 μg/ml kanamycin and 100 μg/ml clonNAT, sporulated, and dissected. Haploid double mutants resistant to both drugs were identified.

To screen for *pmr1*Δ phenotypes, 52 96-well plates representing the collection of mutant strains were thawed, and 5 μl of each culture was used to inoculate 200-μl seed cultures grown 18–36 h in synthetic complete (SC) medium at 30°C. Four microliters of each seed culture was then used to inoculate 96-well microtiter plates each containing 200 μl of SC medium with and without addition of either 1.5 mM 1,2-bis(2-aminophenoxy)ethane-*N*,*N*,*N*′,*N*′-tetraacetic acid (BAPTA), 10 mM $MnCl_2$, or 10 μM amiodarone (AMD). Concentrations were chosen based on results from serial dilution experiments showing the greatest difference between wild type (WT) and *pmr1*Δ growth. On each microtiter plate, two wells were reserved for a WT culture and for growth medium alone, representing positive and negative controls, respectively. Growth was monitored after incubation for 19 h at 30°C by measuring $A_{600\ nm}$ on a BMG FLUOstar Optima multimode plate reader with BMG FLUOstar Optima version 1.20 software (BMG Labtechnologies, Durham, NC). Immediately before recording, cultures were rapidly resuspended using an electromagnetic microtiter plate shaker (Union Scientific, Randallstown, MD), and all recordings were made at 30°C. $A_{600\ nm}$ values were background subtracted and normalized to average WT growth (mean calculated from 52 separate cultures spanning all microtiter plates per screen). Strains showing <20% of WT growth (<1% of the collection) under control conditions (SC) were omitted from further analysis. Of the strains that were included, low $A_{600\ nm}$ values of the seed cultures did not correlate with growth defects observed under experimental conditions. For each screen, conditional growth values were normalized to $A_{600\ nm}$ values obtained under control conditions to estimate sensitivity or tolerance. Data were organized, plotted, and analyzed using Excel X (Microsoft, Redmond, WA), S-Plus 6.2 (Insightful, Seattle, WA), and SPSS 12.0 (SPSS, Chicago, IL) software.

Using the *M*unich *I*nformation center for *P*rotein *S*equences (MIPS) database (http://mips.gsf.de/projects/funcat), we acquired the annotated *Fun*ctional *Cat*egorization (Fun Cat) and *Cell*ular *Loc*ation (Cell Loc) of genes identified in the phenocopy screens. Resulting data from all screens were integrated and visualized as network diagrams by using Osprey network visualization software http://biodata.mshri.on.ca/osprey/servlet/Index. Illustrations were created using Adobe Illustrator CS software (Adobe Systems, Mountain View, CA).

^{45}Ca Uptake

Total cellular accumulation of calcium was measured by growing yeast to logarithmic phase in SC media, followed by harvesting and resuspending in fresh SC media (~3×10^7 cells/ml) supplemented with tracer quantities of $^{45}CaCl_2$ (26.1 μCi/ml). After 2 h of incubation at 30°C, in the absence or presence of the indicated amounts of drugs, cells were harvested rapidly by filtration on to nitrocellulose membrane filters (HAWP, 0.45 μm; Millipore, Billerica, MA), washed with ice-cold wash buffer (10 mM HEPES and 150 mM KCl), placed in scintillation vials, and processed for liquid scintillation counting by using CytoScint scintillation cocktail (MP Biomedicals, Aurora, OH).

Vacuole Staining and Microscopy

Vacuolar accumulation of quinacrine was examined as described previously (Roberts *et al*., 1991). Briefly, ~3×10^7 log-phase yeast cells were harvested and resuspended in 500 μl of YPD buffered with 50 mM Na_2HPO_4, pH 7.6, containing 200 μM quinacrine. After incubation at room temperature for 5 min, cells were sedimented at 10,000 × *g* for 5 s, washed once with 500 μl of 2% glucose buffered with 50 mM Na_2HPO_4, pH 7.6, and resuspended in 100 μl of the same solution. Samples were applied to a microscope slide and viewed immediately in the fluorescence microscope by using a fluorescein filter. To stain with *N*-(3-triethylammoniumpropyl)-4-(*p*-diethylaminophenylhexatrienyl) pyridinium dibromide (FM4-64), yeast cells were grown to logarithmic phase in YPD, and 16 μM FM4-64 (Invitrogen) was added from a stock solution in dimethyl sulfoxide (DMSO) for 30 min. Samples were applied to a microscope slide and viewed immediately in the fluorescence microscope by using a Texas Red filter.

RESULTS AND DISCUSSION

Pmr1 Mutants Show Multiple Drug-sensitive Phenotypes That Arise from Calcium Homeostasis Defects

The best-known growth phenotypes of *pmr1* mutants are directly related to cellular Ca^{2+} or Mn^{2+} homeostasis, as expected for the loss of a Ca^{2+}, Mn^{2+}-transporting ATPase. Thus, *pmr1*Δ strains are hypersensitive to removal of divalent cations from the medium by the chelator BAPTA. We have shown that BAPTA sensitivity in *pmr1* mutants corresponds to calcium starvation in the early part of the secretory pathway and that it can be complemented by heterologous expression of phylogenetically diverse Ca^{2+}-ATPases of the endoplasmic reticulum (ER), plasma membrane, or Golgi subtypes (Ton *et al*., 2002). Likewise, hypersensitivity of *pmr1* strains to high $MnCl_2$ corresponds to accumulation of toxic levels of cellular Mn^{2+} and can be corrected specifically by Mn^{2+}-transporting pumps unique to the Golgi subtype, including human SPCA1 and SPCA2. The recent observation that *pmr1* mutants are sensitive to the antifungal agent amiodarone (Gupta *et al*., 2003) prompted us to search the database for other reports of drug sensitivities. We found that *pmr1* was identified in genome-wide screens of the yeast deletion library for hypersensitivity to wortmannin, tunicamycin, and sulfometuron (Zewail *et al*., 2003; Parsons *et al*., 2004). These drugs target diverse and unrelated cellular pathways: wortmannin is an inhibitor of PI-4 kinase in yeast, tunicamycin blocks protein glycosylation, sulfometuron targets branched chain amino acid synthesis, and amiodarone, an antiarrhythmic agent, has been proposed to cause calcium-mediated cell death in yeast.

To evaluate whether the multiple drug-sensitive phenotypes associated with *pmr1* null mutants arose from loss of Ca^{2+} or Mn^{2+} transport, or both, we made use of a previously described Pmr1 mutant that has an ion-selective defect. Mutant Q783A was shown to retain ^{45}Ca transport and Ca^{2+}-ATPase activity at nearly wild-type levels but was severely attenuated in all Mn^{2+}-dependent functions examined previously (Mandal *et al*., 2000). We introduced Q783A mutant and wild-type *PMR1* genes into yeast strain K616 (*pmr1*Δ*pmc1*Δ*cnb1*Δ; Cunningham and Fink, 1994), which shows robust ion-sensitive growth phenotypes, and we assessed drug sensitivity of the strains (Figure 1). As expected, wild-type Pmr1 improved growth, relative to the vector control, under all conditions tested. Mutant Q783A could not correct Mn^{2+} hypersensitivity of the host strain, but it improved growth in BAPTA similar to wild type (Figure 1, A and B), demonstrating the Mn^{2+}-selective defect of this mutant. We show that expression of mutant Q783A complements drug hypersensitivity to wild-type (amiodarone; Figure 1C), or nearly wild-type levels (sulfometuron methyl, wortmannin, and tunicamycin; Figure 1, D–F), suggesting that Ca^{2+} transport plays a major role in mediating the

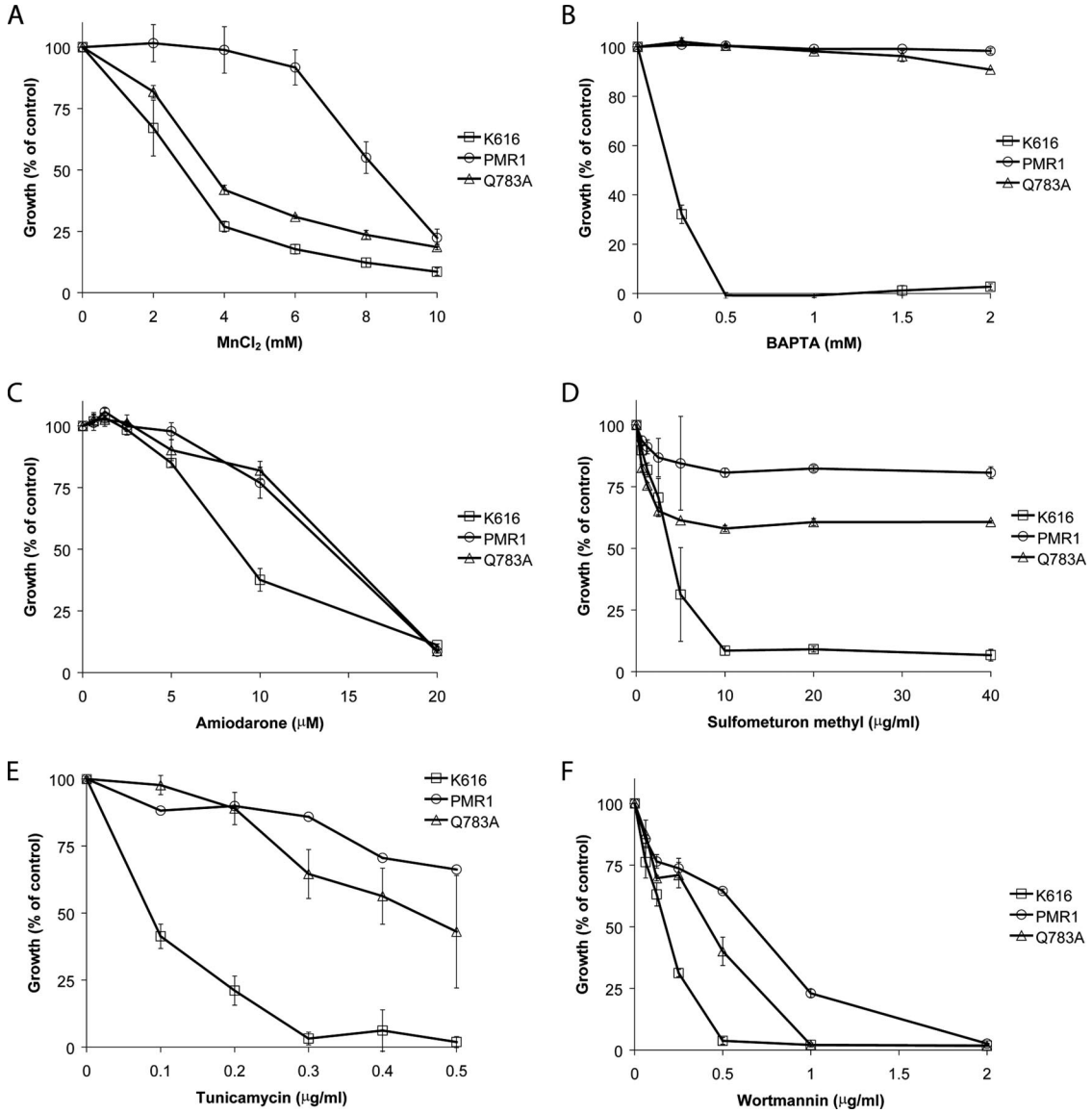

Figure 1. Ion specificity of *pmr1*Δ growth phenotypes. K616 (*pmr1*Δ *pmc1*Δ *cnb1*Δ) was transformed with a *CEN* plasmid carrying *URA3* alone (K616), wild-type ScPmr1 (PMR1), or ScPmr1 with Q783A mutation (Q783A). Cells ($OD_{0.025}$) were cultured overnight in 1 ml of SC medium supplemented with varying concentrations of $MnCl_2$ (A), BAPTA (B), amiodarone (C), sulfometuron methyl (D), tunicamycin (E), or wortmannin (F). Growth, expressed as percentage of control (without drug addition), was measured at OD_{600} and subtracted from background. Every data point is an average of four replicates. Plots are representative of at least two different experiments.

requirement for Pmr1 in the cellular response to multiple drugs. We note that partial complementation by mutant Q783A in tunicamycin (Supplemental Figure 1) is consistent with a role for both Ca^{2+} and Mn^{2+} ions; thus, tunicamycin leads to accumulation of unfolded proteins, a form of cell stress known to require Ca^{2+} ions (Bonilla *et al.*, 2002), however, tunicamycin toxicity may be exacerbated by depletion of Mn^{2+} ions from the Golgi, because endoglycosidases are Mn^{2+}-requiring enzymes. Similarly, there may be overlapping requirements for Ca^{2+} and Mn^{2+} in other drug responses. A potential target, the ATM kinase, mutated in human ataxia telangiectasia, is a Mn^{2+}-requiring enzyme that is sensitive to wortmannin (Chan *et al.*, 2000). These observations underscore the importance of Pmr1-mediated ion homeostasis in multiple cellular pathways that impact drug sensitivity.

Calcium influx has been reported in response to various forms of cell stress (Bonilla *et al.*, 2002; Matsumoto *et al.*, 2002). Therefore, we postulated that drug hypersensitivity in *pmr1* mutants might arise from defective Ca^{2+} homeostasis after drug-induced Ca^{2+} influx. Consistent with this hypothesis, we show that addition of amiodarone, wortmannin, or tunicamycin elicit substantive increase in ^{45}Ca uptake in both wild-type and *pmr1* mutants (Figure 2). We note that basal levels of ^{45}Ca uptake in *pmr1*Δ yeast are higher than wild type in response to depletion of internal stores, as reported previously (Halachmi and Eilam, 1996; Locke *et al.*, 2000). Although addition of sulfometuron did not elicit consistent increases in Ca^{2+} influx over the same period, increasing the drug concentration or time of incubation resulted in higher levels of Ca^{2+} influx (Yadav and Rao, unpublished data). We conclude that drug-induced Ca^{2+}

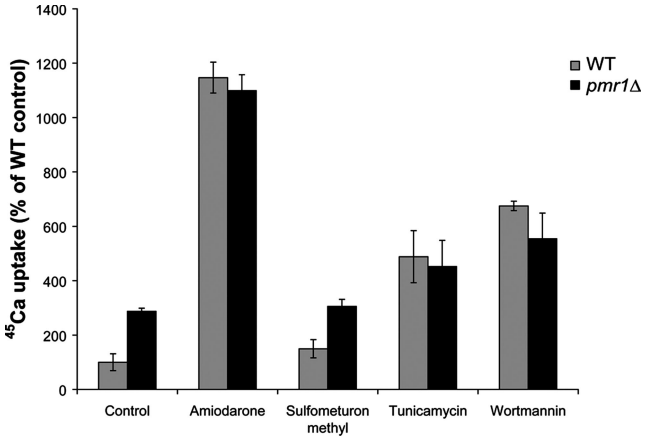

Figure 2. Drug stress induces ^{45}Ca uptake. ^{45}Ca accumulation was measured in whole cells after 2-h incubation with $^{45}CaCl_2$ and the appropriate drug as follows: 40 μM amiodarone, 100 μg/ml sulfometuron methyl, 1 μg/ml tunicamycin, and 0.25 μg/ml wortmannin), as described under *Materials and Methods*. The total counts are expressed as percent normalized to the no drug control of BY4742 (WT). Data are averages of quadruplicates and representative of two independent experiments.

Table 1. Genes sharing two or more of six pmr1Δ growth phenotypes, including hypersensitivity to amiodarone, wortmannin, tunicamycin, sulfometuron methyl, $MnCl_2$, and BAPTA

Phenotype	Genes
6	*PMR1, HUR1, VMA5, YKL118w*
5	*VMA2, HAF4/SNF5*
4	*TFP3/VMA11, VMA13, VMA7, VMA4, VMA12, SNF6*
3	*VMA8, VMA10, VMA22, REF2, ERG2, ERG6, LEM3, GRR1, SPT20, GAL11, SNF8, LOC1, DST2, SAC1, VPS52, VPS45, YDJ1, YGL024w, YJL175w, YBR267w, YLR322w*
2	*CUP5/VMA3, VMA6, CDC50, PDR5, ERG3, ERG4, SEC28, VAM6, COG5, RCY1, SNF7/VPS32, DID4/VPS2, VPS51, VPS54, VPS16, TLG2, VTS1, ARF1, CHC1, SHP1, CNB1, YKR029C, CKI3, ZUO1, SNF2, PER1, IRE1, UBP3, NDE1, URE2, MOG1, SPC72, BUD25, PRS3, STP22, SLG1, IES6, YOR199W, AGP2, AKR1, SIT4, NHP10, RPN4, GPH1, SPT3, GIT2, RPL20B, TOM37, GCN4, HOC1, SIN4, RPL34B, OPI1, RAD18, FEN1, SRO7, YML095C-A, LEA1, HOF1, AAT2, YLR426W, ADA1, ADA4, YGR272C, NAB1, YGL218W, EAP1, GLY1, LPP1, BUD31, MLF3, YPR114W, YER119C-A, PTC4, PCL9, RTT103, STP1, DHH1, PEX17, TAT1, BAP2, YOL162W, RPL23B, SHE3, DLD2*

influx could contribute, at least in part, to the Ca^{2+}-related drug sensitivity of the *pmr1* strain.

Genome-wide Screens for Multiple pmr1Δ Growth Phenotypes Are Enriched in Specific Cellular Pathways

To find specific components and functional modules that operate within the same or parallel cellular pathways as Pmr1, we sought to identify genes that shared multiple *pmr1* mutant phenotypes. Gene deletions resulting in hypersensitivity to wortmannin, tunicamycin, and sulfometuron have been reported, and a partial gene list for amiodarone hypersensitivity has been identified previously (Gupta *et al*., 2003; Zewail *et al*., 2003; Parsons *et al*., 2004). We therefore undertook genome-wide screens of the BY4742 haploid yeast deletion library (~4800 strains) to find additional mutants sensitive to 10 μM amiodarone as well as to 1.5 mM BAPTA and 10 mM $MnCl_2$. Null mutant strains that were similar to, or more sensitive than *pmr1*Δ, in the growth response to each condition were identified and categorized according to function. Each test condition elicited a unique growth response of the deletion collection, characterized by enrichment of distinct functional categories. For example, genes involved in cell rescue and virulence were enriched 1.5-fold in the BAPTA- and amiodarone-sensitive screens ($p = 0.025$) but not in $MnCl_2$, whereas a similar enrichment was seen for cell communication in BAPTA and $MnCl_2$ screens but not in amiodarone. Certain functional categories showed significant, albeit modest, trends of overrepresentation in all six screens; these categories included cellular transport, protein fate, and interaction with the cellular environment (1.25- to 1.75-fold). We reasoned that if these categories were specifically related to Pmr1 function, then the trends observed in individual screens would be further enhanced in the set of genes that share multiple *pmr1* phenotypes. We identified 118 of a total of 695 genes (17%) that shared at least two common growth sensitivities with *pmr1*Δ, and 34 of these (5% of total) shared three or more common phenotypes (Table 1). Graphical representation of functional categories (Figure 3A) in the set of genes sharing three or more phenotypes (≥3, outer ring) and two or more phenotypes (≥2, middle ring) relative to the yeast proteome (inside ring) reveals statistically high enrichment of categories that showed relatively modest changes in the individual phenotype sets. Thus, the ≥2 data set showed enrichment in the categories of protein fate by 1.33-fold ($p = 1.35 \times 10^{-5}$), cell transport by 1.75-fold ($p = 9.2 \times 10^{-10}$), and interaction with cellular environment by 2-fold ($p = 5.56 \times 10^{-8}$). The latter two functions showed even further enhancement, to 2- and 3.25-fold respectively, among genes in the ≥3 data set. Within broad functional categories, certain subcategories showed highly significant enrichment, e.g., the unfolded protein response and ER quality control (5 of a genome-wide pool of 69; $p = 4.81 \times 10^{-3}$) and biogenesis of the vacuole (5 of 44 proteins; $p = 6.38 \times 10^{-4}$).

Similarly, Figure 3B shows the subcellular distribution of gene products represented in the ≥2 and ≥3 phenocopy data sets, relative to the yeast proteome. Here, we observed prominent, statistically significant overrepresentation of proteins localizing to secretory and vacuolar pathways. This included the endoplasmic reticulum, which was enriched from 6% in the proteome to 11 and 15% (up to 2.5-fold), Golgi (up to 4-fold), transport vesicles (up to 4-fold) and vacuole (up to 8-fold). Thus, this analysis reveals that the major cellular pathways responsive to perturbations in ion homeostasis and drug toxicity localize to the endomembrane system.

Of the gene deletions displaying at least two *pmr1* phenotypes (Table 1), only three shared all six drug and ion-related growth sensitivities with *pmr1*Δ: of these three phenotypes, *HUR1* is a dubious open reading frame (ORF) encoded on the opposite strand to that of *PMR1*, so that *hur1*Δ essentially recapitulates *pmr1*Δ. Expression of *HUR1* has not been detected at transcript or protein level, and it has no recognizable orthologues. Because reintroduction of *PMR1* complements all six phenotypes (Figure 1), *HUR1* represents a false positive of the screening strategy; however, it serves as an internal control and validates our findings. Deletion of *VMA5*, encoding a subunit of the vacuolar H^+-ATPase complex, also shares all six growth phenotypes with *pmr1*. *YKL118w* is a dubious ORF that over-

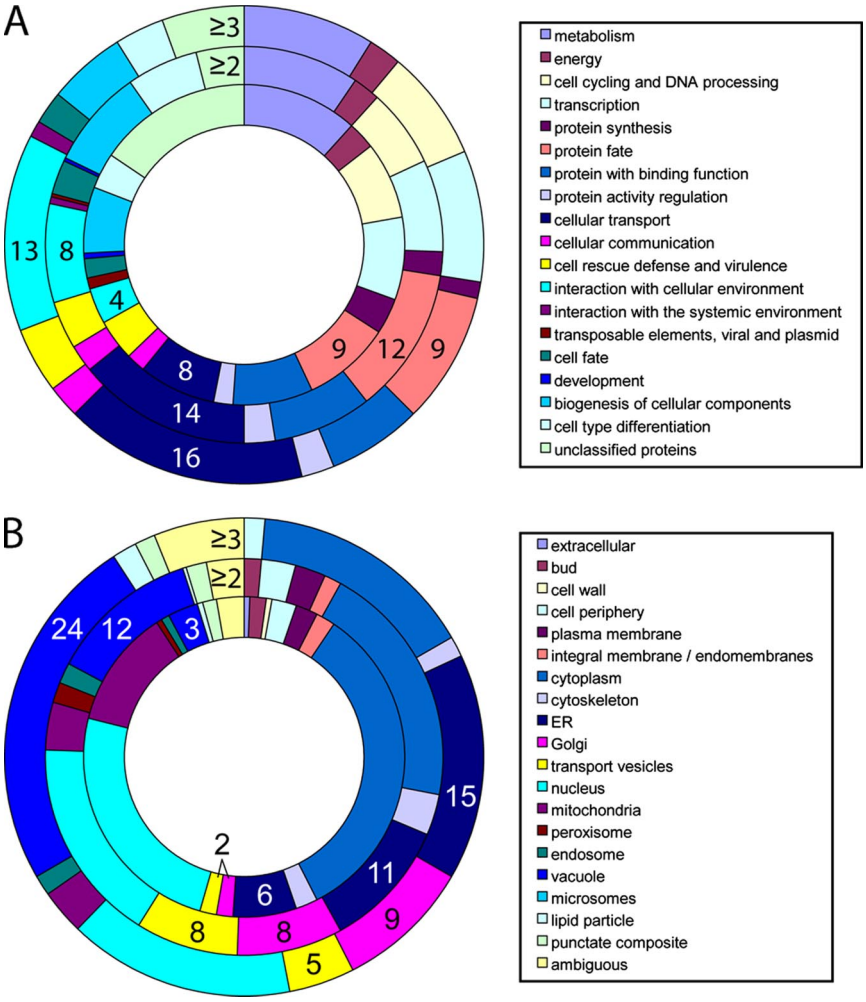

Figure 3. Cell function and location of gene deletions that phenocopy *pmr1*Δ. Graphical representation of genes that share three or more (≥3, outer ring; 34 genes) or two or more (≥2, middle ring; 118 genes) of six *pmr1*Δ growth sensitivities relative to the entire yeast proteome (inside ring; ~6300 genes) classified by function (A) or cellular localization (B). Categories significantly enriched are indicated with numbers that represent the percentage of total genes in that data set.

laps another subunit of the V-ATPase on the opposite strand, that of *VMA12/VPH2*. In all, 12 of the 18 known VMA subunits and assembly factors shared two or more knockout phenotypes with *pmr1*Δ: *VMA5*, *VMA2*, *TFP3/VMA11*, *VMA13*, *VMA7*, *VMA4*, *VMA12*, *VMA8*, *VMA10*, *VMA22*, *VMA6*, and *CUP5/VMA3*, making this the single-most significant functional module of the collective phenotypes. We note that the shared multidrug sensitivity of *pmr1*Δ and *vma*Δ mutants was recently extended to DNA damaging agents, including cisplatin and hydroxyurea (Pan *et al.*, 2006; Liao *et al.*, 2007).

Remarkably, chromatin remodeling complexes were also abundantly represented (Table 1). This included three components of the SWI/SNF nucleosome-remodeling complex (*HAF4/SNF5*, *SNF6*, and *SNF2*) and five subunits of the SAGA/ADA histone acetyltransferase coactivator complex (*GCN5/ADA4*, *SPT20/ADA5*, *ADA1*, *SPT3*, and *SPT7/GIT2*). Two other knockouts would also result in disruption of SWI/SNF components: *YJL175w* overlaps with *SWI13* on the opposite strand, and *YLR322w* is a dubious ORF that would disrupt *SFH1*, a SNF5 homolog. Also included in this functional category are SET3, a histone deacetylase, and NHP10, which is related to mammalian high-mobility group proteins and a likely component of the INO80 ATP-dependent chromatin remodeling machinery. Together with transcription factors (*GAL11*, *SIN4*, *GCN4*, *OPI1*, and *RPN4*), these are likely to represent cellular stress response pathways. There is evidence that the SAGA complex is required for the expression of roughly 10% of the genome that is involved in stress response (Huisinga and Pugh, 2004; van Voorst *et al.*, 2006). Our findings indicate that although ion stress (Ca^{2+}, Mn^{2+}, or H^{+}) and diverse cytotoxic drugs (amiodarone, wortmannin, sulfometuron, or tunicamycin) may target different pathways, they converge to elicit similar downstream cell survival responses.

Multiple genes in the ergosterol biosynthesis pathway, including *ERG2*, *ERG3*, *ERG4*, *ERG6*, and *SAC1*, encoding a lipid inositol phosphoinositide phosphatase, were found to share two or more knockout phenotypes with *PMR1*. These genes would be expected to impact membrane integrity and permeability not only by altering lipid composition but also by affecting the activity of ion and drug transporters as well as protein and vesicular trafficking pathways. Indeed, the latter were represented by genes directing traffic to or from compartments of the Golgi, endosomes, and vacuole (*VPS45*, *VPS51*, *VPS52*, *VPS54*, *SNF8/VPS22*, *SNF7/VPS32*, and *COG5*).

Notably missing from the list of gene mutations that phenocopy *pmr1*Δ were known Ca^{2+} transporters (*PMC1*, *VCX1*) and Ca^{2+} channels (*CCH1*, *MID1*, *YVC1*), pointing to a distinct, nonredundant cellular role of Pmr1. Although large, compensatory increases in expression of Pmc1, the vacuolar ATP-driven Ca^{2+} pump, have been reported (Marchi *et al.*, 1999; Locke *et al.*, 2000), *pmr1* mutants retain distinct phenotypes. This may be because of the unusual ion selectivity of Pmr1,

which transports both Mn^{2+} and Ca^{2+} ions, and more importantly, its unique localization in the Golgi.

pmr1Δ Mutants Maintain Normal Vacuolar pH Despite Aberrant Vacuolar Morphology

Because the vacuolar ATPase has to traffic through the early secretory pathway and Golgi, where Pmr1 activity is important, we considered the possibility that the V-ATPase was dysfunctional in *pmr1* mutants, resulting in overlapping *vma* and *pmr1* phenotypes. The diagnostic test for loss of acidic vacuoles is the inability to grow at alkaline pH or to handle calcium stress at alkaline pH, as seen for *vma5*Δ (Figure 4, A and B). However, *pmr1*Δ was similar to wild type in the growth response to alkaline pH and high calcium (Figure 4, A and B), suggesting that vacuolar pH was normal in this mutant. In *vma* mutants, a consequence of defective acidification within a post-Golgi endosomal compartment is the failure to load the multicopper oxidase Fet3 with copper, resulting in iron starvation and growth sensitivity to the iron-specific chelating agent bathophenanthroline disulfonate (BPS) (Davis-Kaplan *et al*., 2004). We show that the *pmr1* mutant is not hypersensitive to BPS, indicating that loss of the Golgi Ca^{2+}, Mn^{2+} pump does not significantly affect the pH-dependent transport and availability of copper to Fet3 (Figure 4C). Furthermore, vacuoles of wild-type and *pmr1*Δ cells readily took up the fluorescent weak base quinacrine, which becomes protonated and trapped within acidic compartments (Figure 5, A and B). In contrast, the *vma5*Δ mutant failed to accumulate quinacrine, characteristic of defective vacuolar acidification (Figure 5C). However, quinacrine labeling did reveal aberrant vacuolar morphology in the *pmr1* mutant, as has been reported previously (Kellermayer *et al*., 2003). This was more readily visualized using the vacuolar membrane dye FM4-64 (Figure 6), which showed the appearance of multiple vacuolar lobes or fragmented vacuolar compartments in *pmr1*Δ, suggesting a membrane fusion defect. Interestingly, addition of amiodarone caused a rapid fusion of these compartments, resulting in a single large vacuole within a few minutes (Figure 6C). We hypothesized that the amiodarone-induced calcium burst (Courchesne and Ozturk, 2003; Gupta *et al*., 2003) promoted membrane fusion of *pmr1*Δ vacuoles. Consistent with this idea, addition of 5 mM $CaCl_2$ also promoted vacuolar fusion in the *pmr1*Δ mutant (Figure 6D). We conclude that despite the aberrant vacuolar morphology, the *pmr1* mutant has normal vacuolar pH and pH-related vacuolar functions.

Alternatively, could the V-ATPase be required for normal localization or transport activity of Pmr1? We found that distribution of green fluorescent protein-tagged Pmr1 was similar in wild-type and *vma* mutant strains (Ton and Rao, unpublished data). Furthermore, concanamycin A, a specific inhibitor of V-ATPase activity, and protonophores do not inhibit ^{45}Ca uptake by Pmr1 in purified Golgi vesicles (Sorin *et al*., 1997). Finally, detailed kinetic analyses of mammalian orthologues of Pmr1 confirm an absence of pH effects on ATPase activity (Dode *et al*., 2006). Thus, a proton gradient is not directly required for Pmr1 activity. These biochemical observations suggest that the ion transport activities of Pmr1 and V-ATPase do not directly influence each other but that they are required in parallel for the same cellular function.

Synthetic Growth Defect of pmr1 and vma Mutants Point to Parallel, Additive Roles

Genes that share multiple knockout phenotypes with *pmr1*Δ may lie within the same pathway, or they may function in parallel pathways that achieve the same cellular outcome. A straightforward approach to differentiate between these two possibilities is to test for synthetic fitness defects in double null mutants. We show that disruption of both *PMR1* and *VMA* genes leads to severe synthetic fitness defects. Although all spores derived from tetrads in these crosses were able to germinate, the double null mutants of *PMR1* and either *VMA2* or *VMA5* were much smaller in size (Supplemental Figure 2) and grew poorly (Figure 7, A and B). In contrast, a double null mutant of *PMR1* and *SNF6*, a component of the chromatin remodeling complex, showed no synthetic growth defect (Figure 7C). These genetic data cor-

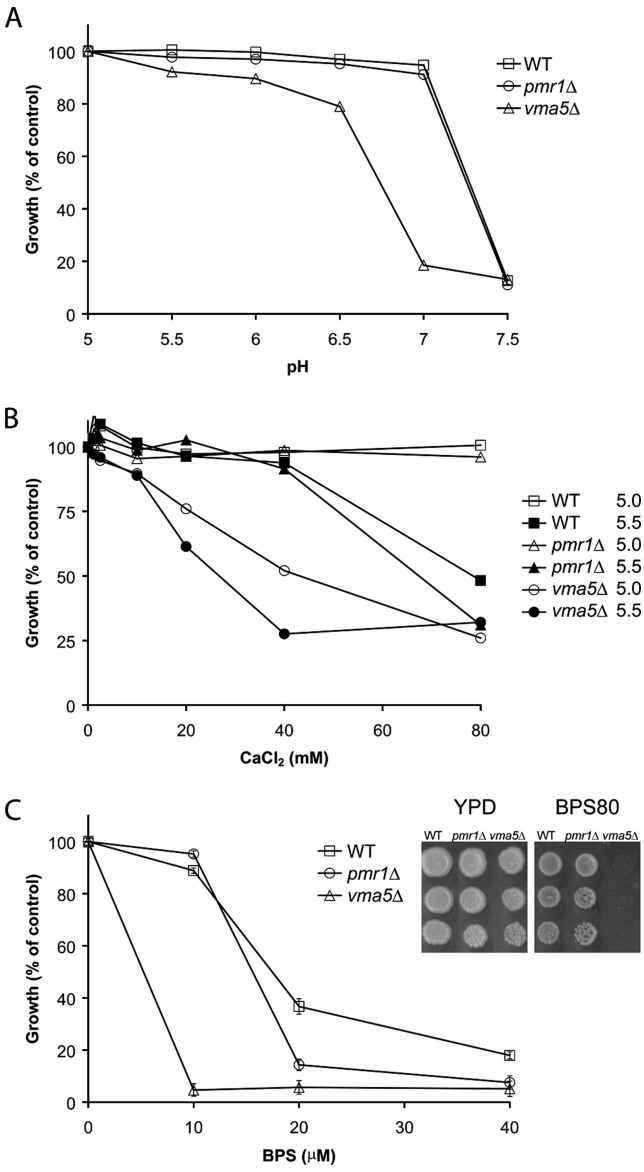

Figure 4. The *pmr1*Δ mutant does not have pH-related growth defects. Alkaline sensitivity was compared in isogenic BY4742 (WT), *pmr1*Δ and *vma5*Δ strains cultured overnight in minimal media buffered to the indicated pH with 50 mM 2-(*N*-morpholino)ethanesulfonic acid/Tris (A) or with added $CaCl_2$ in media buffered to pH 5 or 5.5 (B). Growth was measured as OD_{600} and expressed as percentage of pH 5 (A) or no $CaCl_2$ (B). Data are the average of two replicates. In C, iron deficiency was evaluated by measuring growth in liquid SC medium supplemented with the Fe-specific chelator BPS (graph) or by drop tests in YPD medium supplemented with 80 μM BPS where indicated (inset). The graph shows the average of quadruplicate determinations and the inset shows serial dilutions of 1:5.

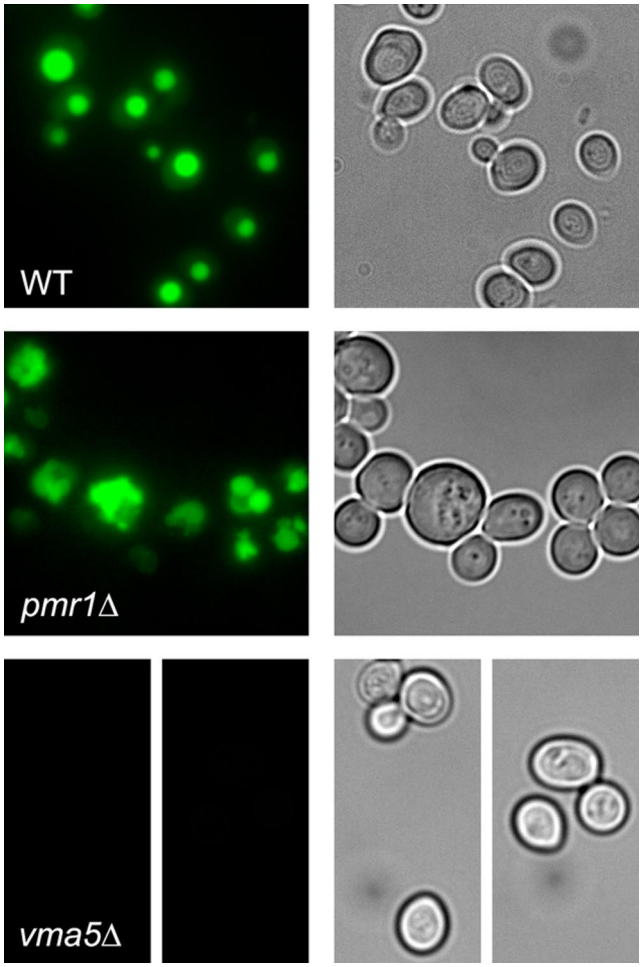

Figure 5. Quinacrine staining of vacuoles is defective in *vma5*Δ but not *pmr1*Δ. Cells were incubated with quinacrine for 5 min, as described under *Materials and Methods*. Micrographs of cell fluorescence (left) and phase contrast (right) show normal pH-dependent uptake of quinacrine in vacuoles of wild-type (WT) and *pmr1*Δ yeast, whereas *vma5*Δ vacuoles fail to accumulate the dye.

roborate our biochemical and phenotypic findings to show that Pmr1 and V-ATPase work in parallel toward a common cellular function.

Functional Overlap of PMR1 and VMA May Occur within the Golgi

As a complementary approach to growth fitness tests, we considered other function-based genome-wide screens that have identified a role for Pmr1. Bonangelino *et al*. (2002) identified *pmr1*Δ as one of 362 mutant strains (7.8% of the viable diploid deletion collection) that were impaired in the

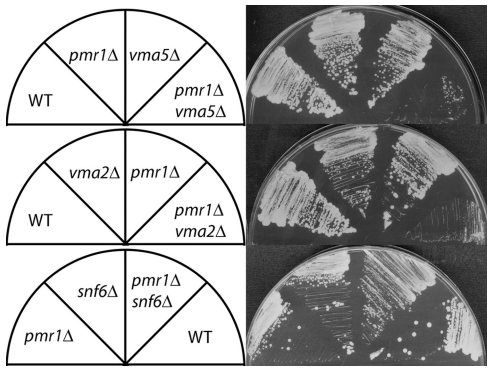

Figure 7. Synthetic fitness defect of *pmr1*Δ *vma*Δ double mutants. Double null mutants of *PMR1* with *VMA2*, *VMA5* and *SNF6* were generated using a *NAT* replacement protocol. After sporulation, mutants were plated on YPD for comparison of growth fitness. Compared with the individual null mutants, *pmr1*Δ*snf6*Δ showed no synthetic growth defect, whereas both *pmr1*Δ*vma5*Δ and *pmr1*Δ*vma2*Δ grew poorly. Data are representative of haploid progenies dissected from 20 tetrads for each cross.

biosynthetic sorting of the vacuolar hydrolase carboxypeptidase Y (CPY), resulting in various levels of inappropriate secretion into the culture medium. This data set is enriched in vacuolar protein sorting (VPS) genes, as well as numerous other genes involved in regulating the actin cytoskeleton, glycosylation and other Golgi functions (Bonangelino *et al*., 2002). Durr *et al*. (1998) have demonstrated that CPY secretion in *pmr1*Δ yeast is a consequence of defective Ca^{2+} homeostasis, because addition of extracellular Ca^{2+}, but not Mn^{2+}, could correct this defect. We also took advantage of a genome-wide screen for defective mannosyl-phosphorylation in the outer layer of the yeast cell wall, which was performed by assaying the haploid deletion collection for decreased binding of the cationic dye Alcian Blue (Conde *et al*., 2003; Corbacho *et al*., 2005). Among the most severely attenuated of 198 low dye binding (*ldb*) mutants identified (4% of the collection), *pmr1/ldb1* also showed the greatest reduction in size of secreted invertase, indicative of defective chain growth (Olivero *et al*., 2003). These phenotypes are likely to be a consequence of Mn^{2+} insufficiency within the Golgi of the *pmr1* mutant, because endoglycosidases are Mn^{2+}-requiring enzymes. Indeed, underglycosylation of invertase in *pmr1* can be corrected by supplementing the growth medium with Mn^{2+} but not Ca^{2+} (Durr *et al*., 1998). Like the CPY screen, the *ldb* mutants fell into diverse cellular pathways; however, we note that secretory and vacuolar trafficking pathways within the cell were abundantly represented. Figure 8 is a Venn diagram showing the extent of overlap between the pool of genes sharing at least two, and up to six, *pmr1* phenotypes and the functional screens for CPY secretion and low dye binding. Common to all three data sets were 22 genes: in addition to *PMR1*, this included

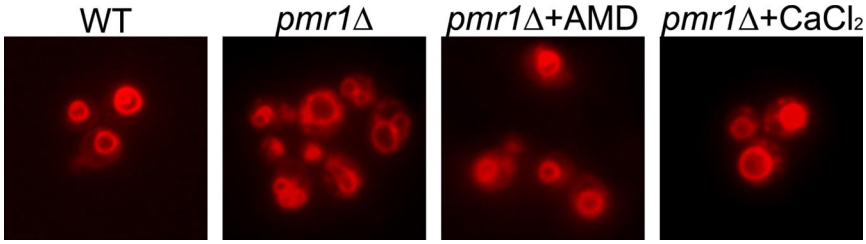

Figure 6. Aberrant morphology of vacuolar compartments in *pmr1*Δ can be corrected by Ca^{2+} influx. Fluorescence micrographs show FM4-64 staining of WT (BY4742) and *pmr1*Δ cells. Vacuoles in *pmr1*Δ have a fragmented appearance relative to wild type. Incubation with 40 μM AMD or 5 mM $CaCl_2$ for 5 min elicits fusion of the smaller compartments into a single large vacuole with some FM4-64 staining fragments remaining.

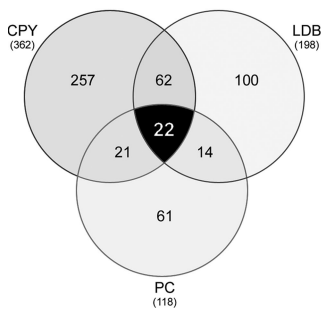

V-ATPase	Golgi
VMA2	PMR1
VMA3	HOC1
VMA4	**Trafficking**
VMA5	VPS15
VMA6	VPS45
VMA7	VPS54
VMA8	COG5
VMA10	**Other**
VMA11	SHP1
VMA12	REF2
VMA13	PER1
VMA22	HOF1

Figure 8. Shared *pmr1*Δ and *vma*Δ phenotypes are enriched for Golgi-localized functions. Venn diagram representing overlap between *pmr1*Δ phenocopy screen (PC; this work), functional screens for secretion of CPY (Bonangelino *et al*., 2002) and low dye binding of Alcian Blue (LDB; Corbacho *et al*., 2005). The 22 genes common to all three data sets are listed to the right and include *VMA* and *PMR1* genes, *HOC1* that encodes a mannosyltransferase of the Golgi, and several *VPS* genes involved in Golgi traffic.

12 *VMA* genes, four genes involved in sorting or fusion of vesicles from or to the Golgi (*VPS15*, *VPS45*, *VPS54*, and *COG5*), and a Golgi-resident mannosyltransferase (*HOC1*). The relationship of the remaining genes to the observed phenotypes is currently not clear. For example, *PER1* encodes an ER-localized protein that has been implicated in remodeling of GPI anchors and their association with raft-like domains, which could in turn impact on Golgi/secretory pathway function (Fujita *et al*., 2006). Overall, a majority of the common genes (18/22) encode proteins known to reside within or traffic to the Golgi membranes, including the V-ATPase that has a distinct, Golgi-localized isoform (Manolson *et al*., 1994; Kawasaki-Nishi *et al*., 2001). It is interesting to note that many members of this group also share a common synthetic lethality with endocytosis genes. For example, *pmr1*Δ, *vma2*Δ, *vps15*Δ, *vps45*Δ, and *vps54*Δ are individually inviable with *end4/sla2*Δ (Munn and Riezman, 1994; Conibear and Stevens, 2000). Together, we suggest that shared phenotypes of *pmr1* and *vma* mutants, including multiple drug and ion sensitivity, derive from shared ion transport functions within the Golgi.

Based on this hypothesis, we asked whether *pmr1* shared additional *vma* phenotypes that may be attributed to Golgi/secretory pathway function. We tested sensitivity to calcofluor white, an antimicrobial agent that binds to chitin on the cell wall. Altered sensitivity to calcofluor white relates to missorting of chitin synthetase and altered levels of chitin on the cell surface, and it is a known phenotype of *vma* mutants (Davis-Kaplan *et al*., 2004). Indeed, we found that like *vma5*Δ, *pmr1*Δ displayed increased sensitivity to calcofluor white (Figure 9A). Another *vma* phenotype also shared with *pmr1*Δ relates to zinc homeostasis. It has been argued that the acute Zn^{2+} sensitive phenotype of *vma* mutants is due to defective vacuolar sequestration and detoxification of this ion and that this phenotype may serve as a diagnostic test to distinguish vacuolar from pre-vacuolar functions of the V-ATPase. However, we show that *pmr1*Δ mutants are nearly as

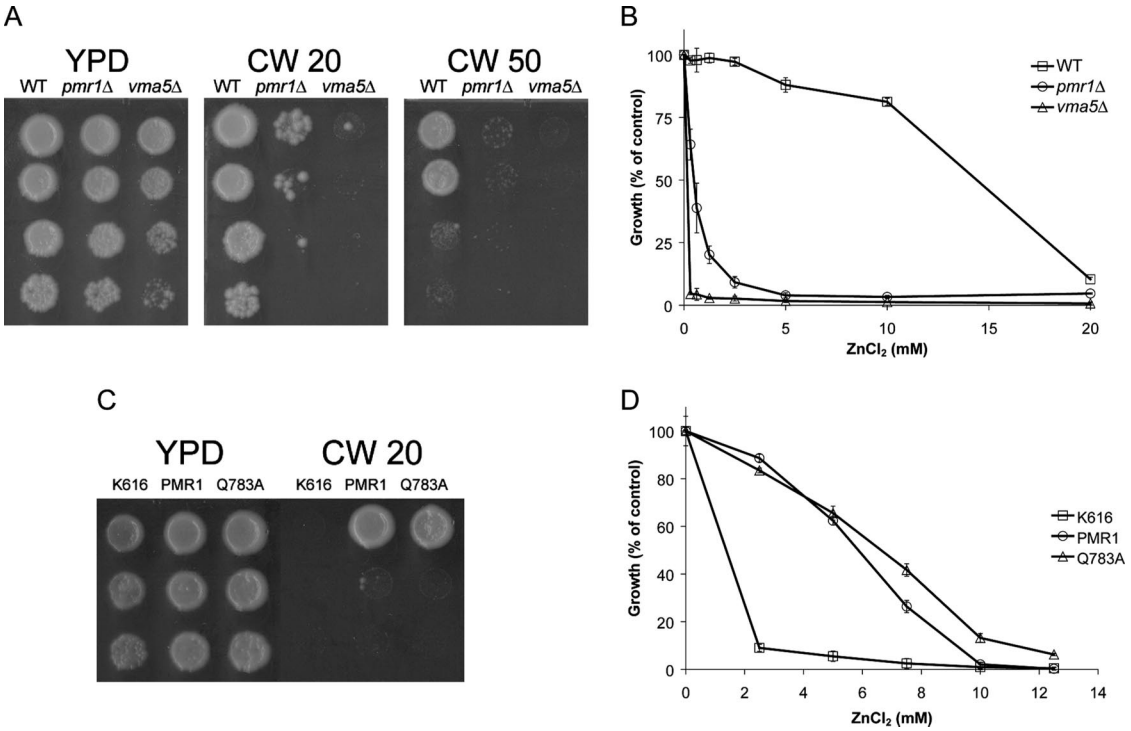

Figure 9. Novel *pmr1*Δ phenotypes of calcofluor white and zinc sensitivity are shared with *vma5*Δ. (A) Growth of yeast strains in the presence of calcofluor white. BY4742 (WT), and isogenic *pmr1*Δ and *vma5*Δ were grown overnight in minimal media and adjusted to 1 OD/ml. Two microliters of fivefold serial dilutions of each strain were spotted on YPD plates supplemented with DMSO as solvent control (YPD), 20 or 50 μg/ml calcofluor white (CW 20 and CW 50, respectively). Growth at 30°C was monitored after 2 d. (B) Zn^{2+} sensitivity of yeast strains. One-milliliter cultures of SC medium supplemented with indicated amounts of $ZnCl_2$ were seeded with $OD_{0.025}$ of cells and incubated at 30°C overnight. Background subtracted growth (OD_{600}) was an average of quadruplicates and is expressed as a percentage of control (no $ZnCl_2$). (C) Calcofluor white sensitivity of strain K616, plated as in A, is complemented by both WT (PMR1) and mutant Q783A. (D) Zn^{2+} sensitivity of K616, monitored as in B, is complemented by both WT (PMR1) and mutant Q783A.

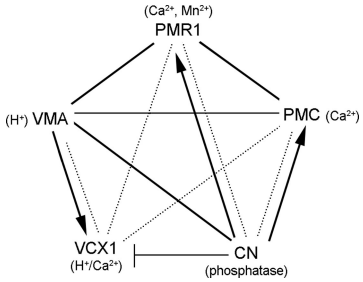

Figure 10. Gene interactions between ion (H^+, Ca^{2+}) transporters and calcineurin. Heavy lines indicate synthetic sick or lethal interactions, and dotted lines indicate absence of any synthetic growth effects between null alleles in standard medium (i.e., absence of added calcium stress). Arrows represent biochemical activation; thus, the V-ATPase provides the H^+ gradient that drives Ca^{2+} uptake by Vcx1, and activated calcineurin mediates transcriptional induction of *PMR1* and *PMC1* genes. See text for details and references.

sensitive to Zn^{2+} as the *vma5*Δ mutant (Figure 9B). Given that *pmr1* mutants have normal pH_v, it is unlikely that Zn^{2+} sensitivity is associated with disruption of vacuolar sequestration of this ion in *pmr1*Δ cells. Therefore, we suggest that it may be due to disruption of a shared role in membrane trafficking within the Golgi or a prevacuolar compartment. We found that both calcofluor white sensitivity (Figure 9C) and Zn^{2+} sensitivity (Figure 9D) of *pmr1*Δ could be fully complemented by the Mn^{2+}-defective Q783A mutant of Pmr1, indicating that these defects are related to Ca^{2+} homeostasis.

A Phenomics Approach Helps Distinguish Vacuolar and Prevacuolar Roles of the Proton Pump

Our finding that *vma* mutants share synthetic fitness defect and multiple phenotypes with the *pmr1* mutant adds one more connecting link to the complex network of gene interactions involved in cellular ion homeostasis (Figure 10). It is known that *vma* mutants have calcium-handling defects and are therefore sensitive to calcium-induced stress. The vacuole is the major reservoir of calcium in the yeast cell, most of it in a nonexchangeable form, presumably complexed with phosphates and other anions. However, if the role of the V-ATPase in Ca^{2+} homeostasis is solely to fuel vacuolar Ca^{2+} uptake and sequestration via H^+-coupled transporters, it is indeed surprising that a mutant lacking Vcx1, the vacuolar H^+/Ca^{2+} exchanger, does not share the multiple drug-sensitive growth phenotypes or trafficking defects described in this work. Moreover, *vcx1* mutants show no synthetic fitness defect with *pmr1* mutants (Cunningham and Fink, 1996). Although it cannot be excluded that there are other, as yet uncharacterized, H^+/Ca^{2+} antiporters, Vcx1 has been shown to be the major transport pathway for low-affinity, high-capacity removal of cytosolic Ca^{2+} (Miseta *et al*., 1999; Forster and Kane, 2000). One explanation is that Vcx1 is redundant with Pmc1, the primary Ca^{2+} pump of vacuolar membrane; however, a *pmc1*Δ*vcx1*Δ mutant is viable (Cunningham and Fink, 1996), although it has added sensitivity to high calcium stress. Double mutants of *vma* genes with *pmc1*Δ, *pmr1*Δ or calcineurin (*cnb1*Δ) show slow growth or no growth even in the absence of calcium stress (Forster and Kane, 2000; this work), consistent with additional prevacuolar/secretory functions of the V-ATPase, separate from a vacuolar role.

There is other evidence that a role for V-ATPase in Ca^{2+} homeostasis is unlikely to be restricted to vacuolar detoxification of excess calcium. Intriguingly, inactivation of *vma* genes in *Neurospora crassa* had dramatic effects on hyphal morphology by restricting hyphal elongation and stimulating branching (Bowman *et al*., 2000). The authors note that when they added the calcium reporter chlortetracycline to *N. crassa*, they saw brightly glowing hyphal tips in wild type but no fluorescence in *vma* null mutants. This points to a disruption of ion homeostasis along the secretory pathway in the *vma* mutants. Consistent with this idea, disruption of the *N. crassa PMR1* gene, but not of other Ca^{2+} pumps and antiporters, resulted in a similar multibranched hyphal morphology (Bowman, B., and Bowman, E. J., personal communication). Many of the shared phenotypes between *pmr1* and *vma* mutants described in this work are directly associated with disruption of the secretory pathway and prevacuolar trafficking pathways (such as calcofluor white sensitivity, low Alcian Blue binding, and CPY secretion). Furthermore, we show that multiple drug- and ion-sensitive growth phenotypes are predominantly associated with disruption of secretory and vacuolar biogenesis pathways (Figure 3).

In mammalian cells, there is experimental evidence for the trafficking and function of V-ATPase along secretory and endocytic pathways to and from the plasma membrane (Breton and Brown, 2007). Although yeast Vma has not been detected at the cell surface, *vma* mutants show markedly reduced rates of endocytosis (Perzov *et al*., 2002). Moreover, there is evidence for a distinct, Golgi-localized isoform of the 100-kDa *a* subunit of the V-ATPase, which contains the Stv1 subunit in place of Vph1, resulting in distinct functional and regulatory properties (Manolson *et al*., 1994; Kawasaki-Nishi *et al*., 2001). In contrast to the multiplicity of subunit isoforms in mammals, Stv1 and Vph1 represent the only V-ATPase subunit isoforms found in fungi, consistent with the importance of distinct Golgi and vacuolar functions of the V-ATPase. Because of the ability of these two subunit isoforms to partially compensate for each other, it has been difficult to separate Golgi-specific phenotypes of the V-ATPase from its vacuolar functions. The phenomic approach used in this study reveals distinct Vma functions that overlap with the Golgi Ca^{2+}, Mn^{2+}-ATPase Pmr1. We suggest that these shared phenotypes provide evidence for secretory pathway and prevacuolar functions of the V-ATPase. Given the excellent conservation of basic ion homeostasis mechanisms from yeast to human (for review, see Ton and Rao, 2005), our findings may be extrapolated to mammalian models. There are examples of defects in tissue-specific isoforms of V-ATPase or Ca^{2+}-ATPase that are known or suspected to give rise to a similar disease phenotype, such as deafness and male sterility (Prasad *et al*., 2004; Breton and Brown, 2007). Calcium and proton homeostasis are also closely linked in normal and pathophysiological conditions; a case in point is osteopetrorickets (Kaplan *et al*., 1993), where defective acidification by V-ATPase leads to osteopetrosis, abnormally high body calcium, and paradoxically, poor calcium incorporation into bone. In conclusion, the overlap of calcium and proton homeostasis pathways, particularly in Golgi and prevacuolar traffic, revealed by a phenomics approach in yeast, may help in understanding and treatment of complex phenotypes associated with disease.

ACKNOWLEDGMENTS

This work was supported by National Institutes of Health grant GM-62142 (to R.R.).

REFERENCES

Bonangelino, C. J., Chavez, E. M., and Bonifacino, J. S. (2002). Genomic screen for vacuolar protein sorting genes in *Saccharomyces cerevisiae*. Mol. Biol. Cell *13*, 2486–2501.

Bonilla, M., Nastase, K. K., and Cunningham, K. W. (2002). Essential role of calcineurin in response to endoplasmic reticulum stress. EMBO J. *21*, 2343–2353.

Bowman, E. J., Kendle, R., and Bowman, B. J. (2000). Disruption of *vma-1*, the gene encoding the catalytic subunit of the vacuolar H^+-ATPase, causes severe morphological changes in *Neurospora crassa*. J. Biol. Chem. *275*, 167–176.

Breton, S., and Brown, D. (2007). New insights into the regulation of V-ATPase-dependent proton secretion. Am. J. Physiol. *292*, F1–F10.

Chan *et al*. (2000). Purification and characterization of ATM from human placenta. A manganese-dependent, wortmannin-sensitive serine/threonine protein kinase. J. Biol. Chem. *275*, 7803–7810.

Cho, J. H., Ko, K. M., Singaravelu, G., and Ahnn, J. (2005). *Caenorhabditis elegans* PMR1, a P-type calcium ATPase, is important for calcium/manganese homeostasis and oxidative stress response. FEBS Lett. *579*, 778–782.

Conde, R., Pablo, G., Cueva, R., and Larriba, G. (2003). Screening for new yeast mutants affected in mannosylphosphorylation of cell wall mannoproteins. Yeast *20*, 1189–1211.

Courchesne, W. E., and Ozturk, S. (2003). Amiodarone induces a caffeine-inhibited, MID1-depedent rise in free cytoplasmic calcium in *Saccharomyces cerevisiae*. Mol. Microbiol. *47*, 223–234.

Conibear, E., and Stevens, T. H. (2000). Vps52p, Vps53p, and Vps54p form a novel multisubunit complex required for protein sorting at the yeast late Golgi. Mol. Biol. Cell. *11*, 305–323.

Corbacho, I., Olivero, I., Hernandez, L. M. (2005). A genome-wide screen for *Saccharomyces cerevisiae* nonessential genes involved in mannosyl phosphate transfer to mannoprotein-linked oligosaccharides. Fungal Genet. Biol. *42*, 773–790.

Cunningham, K. W., and Fink, G. R. (1994). Calcineurin-dependent growth control in *Saccharomyces cerevisiae* mutants lacking PMC1, a homolog of plasma membrane Ca^{2+} ATPases. J. Cell Biol. *124*, 351–363.

Cunningham, K. W., and Fink, G. R. (1996). Calcineurin inhibits VCX1-dependent H^+/Ca^{2+} exchange and induces Ca^{2+} ATPases in *Saccharomyces cerevisiae*. Mol. Cell Biol. *16*, 2226–2237.

Davis-Kaplan, S. R., Ward, D. M., Shiflett, S. L., and Kaplan, J. (2004). Genome-wide analysis of iron-dependent growth reveals a novel yeast gene required for vacuolar acidification. J. Biol. Chem. *279*, 4322–4329.

Dode, L., Andersen, J. P., Vanoevelen, J., Raeymaekers, L., Missiaen, L., Vilsen, B., and Wuytack, F. (2006). Dissection of the functional differences between human secretory pathway Ca^{2+}/Mn^{2+}-ATPase (SPCA) 1 and 2 isoenzymes by steady-state and transient kinetic analyses. J. Biol. Chem. *281*, 3182–3189.

Durr, G., Strayle, J., Plemper, R., Elbs, S., Klee, S. K., Catty, P., Wolf, D. H., and Rudolph, H. K. (1998). The medial-Golgi ion pump Pmr1 supplies the yeast secretory pathway with Ca^{2+} and Mn^{2+} required for glycosylation, sorting, and endoplasmic reticulum-associated protein degradation. Mol. Biol. Cell *9*, 1149–1162.

Foggia, L., and Hovnanian, A. (2004). Calcium pump disorders of the skin. Am. J. Med. Genet. C. Semin. Med. Genet. *131C*, 20–31.

Forster, C., and Kane, P. M. (2000). Cytosolic Ca^{2+} homeostasis is a constitutive function of the V-ATPase in *Saccharomyces cerevisiae*. J. Biol. Chem. *275*, 38245–38253.

Fujita, M., Umemura, M., Yoko-o, T., and Jigami, Y. (2006) *PER1* is required for GPI-phospholipase A_2 activity and involved in lipid remodeling of GPI-anchored proteins. Mol. Biol. Cell *17*, 5253–5264.

Gupta, S. S., Ton, V. K., Beaudry, V., Rulli, S., Cunningham, K., and Rao, R. (2003). Antifungal activity of amiodarone is mediated by disruption of calcium homeostasis. J. Biol. Chem. *278*, 28831–28839.

Halachmi, D., and Eilam, Y. (1996). Elevated cytosolic free Ca^{2+} concentrations and massive Ca^{2+} accumulation within vacuoles, in yeast mutant lacking PMR1, a homolog of Ca^{2+}-ATPase. FEBS Lett. *392*, 194–200.

Huisinga, K. L., and Pugh, B. F. (2004). A genome-wide housekeeping role for TFIID and a highly regulated stress-related role for SAGA in *Saccharomyces cerevisiae*. Mol. Cell *13*, 573–585.

Kaplan, F. S., August, C. S., Fallon, M. D., Gannon, F., and Haddad, J. G. (1993). Osteopetrorickets. The paradox of plenty. Pathophysiology and treatment. Clin. Orthop. Relat. Res. *294*, 64–78.

Kawasaki-Nishi, S., Nishi, T., and Forgac, M. (2001). Yeast V-ATPase complexes containing different isoforms of the 100-kDa *a*-subunit differ in coupling efficiency and in vivo dissociation. J. Biol. Chem. *276*, 17941–17948.

Kellermayer, R., Aiello, D. P., Miseta, A., and Bedwell, D. M. (2003). Extracellular Ca^{2+} sensing contributes to excess Ca^{2+} accumulation and vacuolar fragmentation in a *pmr1*Δ mutant of *S. cerevisiae*. J. Cell Sci. *116*, 1637–1646.

Liao, C., Hu, B., Arno, M. J., and Panaretou, B. (2007). Genomic screening in vivo reveals the role played by Vacuolar H^+ ATPase and cytosolic acidification in sensitivity to DNA damaging agents such as cisplatin. Mol. Pharmacol. *71*, 416–425.

Locke, E. G., Bonilla, M., Liang, L., Takita, Y., and Cunningham, K. W. (2000). A homolog of voltage-gated Ca^{2+} channels stimulated by depletion of secretory Ca^{2+} in yeast. Mol. Cell Biol. *20*, 6686–6694.

Manolson, M. F., Wu, B., Proteau, D., Taillon, B. E., Roberts, B. T., Hoyt, M. A., and Jones, E. W. (1994). STV1 gene encodes functional homologue of 95-kDa yeast vacuolar H^+-ATPase subunit Vph1p. J. Biol. Chem. *269*, 14064–14074.

Mandal, D., Woolf, T. B., and Rao, R. (2000). Manganese selectivity of Pmr1, the yeast secretory pathway ion pump, is defined by residue Gln783 in transmembrane segment 6. Residue Asp778 is essential for cation transport. J. Biol. Chem. *275*, 23933–23938.

Marchi, V., Sorin, A., Wei, Y., and Rao, R. (1999). Induction of vacuolar Ca^{2+}-ATPase and H^+/Ca^{2+} exchange activity in yeast mutants lacking Pmr1, the Golgi Ca^{2+}-ATPase. FEBS Lett. *454*, 181–186.

Matsumoto, T. K., Ellsmore, A. J., Cessna, S. G., Low, P. S., Pardo, J. M., Bressan, R. A., and Hasegawa, P. M. (2002). An osmotically induced cytosolic Ca^{2+} transient activates calcineurin signaling to mediate ion homeostasis and salt tolerance of *Saccharomyces cerevisiae*. J. Biol. Chem. *277*, 33075–33080.

Miseta, A., Kellermayer, R., Aiello, D. P., Fu, L., and Bedwell, D. M. (1999). The vacuolar Ca^{2+}/H^+ exchanger Vcx1p/Hum1p tightly controls cytosolic Ca^{2+} levels in *S. cerevisiae*. FEBS Lett. *451*, 132–136.

Munn, A. L., and Riezman, H. (1994). Endocytosis is required for the growth of vacuolar H^+-ATPase-defective yeast: identification of six new *END* genes. J. Cell Biol. *127*, 373–386.

Olivero, I., Corbacho, I., and Hernandez, L. M. (2003). The *ldb1* mutant of *Saccharomyces cerevisiae* is defective in Pmr1p, the yeast secretory pathway/Golgi Ca^{2+}/Mn^{2+}-ATPase. FEMS Microbiol. Lett. *219*, 137–142.

Pan, X., Ye, P., Yuan, D. S., Wang, X., Bader, J. S., and Boeke, J. D. (2006). A DNA integrity network in the yeast *Saccharomyces cerevisiae*. Cell *124*, 1069–1081.

Parsons, A. B., Brost, R. L., Ding, H., Li, Z., Zhang, C., Sheikh, B., Brown, G. W., Kane, P. M., Hughes, T. R., and Boone, C. (2004). Integration of chemical-genetic and genetic interaction data links bioactive compounds to cellular target pathways. Nat. Biotechnol. *22*, 62–69.

Perzov, N., Padler-Karavani, V., Nelson, H., and Nelson, N. (2002). Characterization of yeast V-ATPase mutants lacking Vph1p or Stv1p and the effect on endocytosis. J. Exp. Biol. *205*, 1209–1219.

Prasad, V., Okunade, G. W., Miller, M. L., and Shull, G. E. (2004). Phenotypes of SERCA and PMCA knockout mice. Biochem. Biophys. Res. Commun. *322*, 1192–1203.

Ramos-Castaneda, J. *et al*. (2005). Deficiency of ATP2C1, a Golgi ion pump, induces secretory pathway defects in endoplasmic reticulum (ER)-associated degradation and sensitivity to ER stress. J. Biol. Chem. *280*, 9467–9473.

Roberts, C. J., Raymond, C. K., Yamashiro, C. T., and Stevens, T. H. (1991). Methods for studying the yeast vacuole. Methods Enzymol. *194*, 644–661.

Rudolph, H. K., Antebi, A., Fink, G. R., Buckley, C. M., Dorman, T. E., LeVitre, J., Davidow, L. S., Mao, J. I., and Moir, D. T. (1989). The yeast secretory pathway is perturbed by mutations in PMR1, a member of a Ca^{2+} ATPase family. Cell *58*, 133–145.

Sorin, A., Rosas, G., and Rao, R. (1997). PMR1, a Ca^{2+}-ATPase in yeast Golgi, has properties distinct from sarco/endoplasmic reticulum and plasma membrane calcium pumps. J. Biol. Chem. *272*, 9895–9901.

Ton, V. K., Mandal, D., Vahadji, C., and Rao, R. (2002). Functional expression in yeast of the human secretory pathway Ca^{2+}, Mn^{2+}-ATPase defective in Hailey-Hailey disease. J. Biol. Chem. *277*, 6422–6427.

Ton, V. K., and Rao, R. (2004). Functional expression of heterologous proteins in yeast: insights into Ca^{2+} signaling and Ca^{2+}-transporting ATPases. Am. J. Physiol. *287*, C580–C589.

Tong, A. H. *et al*. (2001). Systematic genetic analysis with ordered arrays of yeast deletion mutants. Science *294*, 2364–2368.

van Voorst, F., Houghton-Larsen, J., Jonson, L., Kielland-Brandt, M. C., and Brandt, A. (2006). Genome-wide identification of genes required for growth of *Saccharomyces cerevisiae* under ethanol stress. Yeast *23*, 351–359.

Zewail, A., Xie, M. W., Xing, Y., Lin, L., Zhang, P. F., Zou, W., Saxe, J. P., and Huang, J. (2003). Novel functions of the phosphatidylinositol metabolic pathway discovered by a chemical genomics screen with wortmannin. Proc. Natl. Acad. Sci. USA *100*, 3345–3350.